



Neural correlates of binocular depth inversion illusion in antipsychotic-naïve first-episode schizophrenia patients

Cathrin Rohleder^{1,2} · Dagmar Koethe^{3,4} · Stefan Fritze¹ · Cristina E. Topor¹ · F. Markus Leweke^{1,4} · Dusan Hirjak¹

Received: 27 August 2017 / Accepted: 13 March 2018 / Published online: 19 March 2018
© Springer-Verlag GmbH Germany, part of Springer Nature 2018

Abstract

Objectives Binocular depth inversion illusion (BDII), a visual, ‘top–down’-driven information process, is impaired in schizophrenia and particularly in its early stages. BDII is a sensitive measure of impaired visual information processing and represents a valid diagnostic tool for schizophrenia and other psychotic disorders. However, neurobiological underpinnings of aberrant BDII in first-episode schizophrenia are largely unknown at present.

Methods In this study, 22 right-handed, first-episode, antipsychotic-naïve schizophrenia patients underwent BDII assessment and MRI scanning at 1.5 T. The surface-based analysis via new version of FreeSurfer (6.0) enabled calculation of cortical thickness and surface area. BDII total and faces scores were related to the two distinct cortical measurements.

Results We found a significant correlation between BDII performance and cortical thickness in the inferior frontal gyrus and middle temporal gyrus ($p < 0.003$, Bonferroni corr.), as well as superior parietal gyrus, postcentral gyrus, supramarginal gyrus, and precentral gyrus ($p < 0.05$, CWP corr.), respectively. BDII performance was significantly correlated with surface area in the superior parietal gyrus and right postcentral gyrus ($p < 0.003$, Bonferroni corr.).

Conclusion BDII performance may be linked to cortical thickness and surface area variations in regions involved in “adaptive” or “top–down” modulation and stimulus processing, i.e., frontal and parietal lobes. Our results suggest that cortical features of distinct evolutionary and genetic origin differently contribute to BDII performance in first-episode, antipsychotic-naïve schizophrenia patients.

Keywords Depth inversion illusion (DII) · MRI · Schizophrenia · Perception · Cortex · FreeSurfer

Introduction

The depth inversion illusion (DII) reflects a visual information process, resulting in the illusory perception of concave depictions as being convex (e.g., a hollow face is perceived as normal face). A binocular depth inversion

illusion (BDII) can be achieved by presenting three-dimensional (3D) images pseudoscopically (i.e., interchanging the visual information for the right and left eye). The intensity of the illusion depends amongst others on object familiarity, with more familiar objects producing more pronounced DII or BDII [47, 73]. Hence, it has been hypothesized that the perceptual knowledge based on current context and past experiences (“adaptive” or “top–down” process) is able to override stereoscopic cues (“bottom–up process”), resulting in an internal correction of implausible visual information [19, 51, 56, 78]. Interestingly, schizophrenia patients, subjects at ultra-high risk (UHR) for psychosis, as well as healthy individuals after intake of cannabis, dronabinol, or nabilone, perceive BDII or DII to a lesser extent. This led to the hypothesis that the balance of “adaptive” or “top–down” and “bottom–up” processes of perception is disturbed in psychotic states, probably based on weakened “top–down” information processing [19, 22, 47, 51, 52, 54, 55, 73].

✉ Dusan Hirjak
dusan.hirjak@zi-mannheim.de

¹ Department of Psychiatry and Psychotherapy, Central Institute of Mental Health, Medical Faculty Mannheim, Heidelberg University, 68159 Mannheim, Germany

² Institute of Radiochemistry and Experimental Molecular Imaging, University Hospital of Cologne, Cologne, Germany

³ Department of Psychosomatic Medicine and Psychotherapy, Central Institute of Mental Health, Medical Faculty Mannheim, Heidelberg University, Mannheim, Germany

⁴ Brain and Mind Centre, University of Sydney, Sydney, Australia

Overall, it is unclear whether BDII performance relies on a widely distributed cortical network, or whether this test predominantly taps into fronto-parietal regions involved in “adaptive” or “top-down” modulation. Therefore, we investigated cortical features of distinct neurodevelopmental origin (such as cortical thickness and surface area) using surface-based morphometry in antipsychotic-naïve first-episode schizophrenia patients. Surface-based morphometry accounts for cortex abnormalities more specifically than voxel-based morphometry [64, 84] and could help to gain better understanding of the neural correlates underlying impaired BDII in first-episode schizophrenia patients. The aims of the present MRI study were to (1) provide a fine-grained analysis of cortex variations underlying BDII in antipsychotic-naïve first-episode schizophrenia patients and (2) determine whether cortical thickness and surface area variations differentially contribute to aberrant BDII performance in this group of patients. We hypothesized that higher BDII scores would be significantly correlated with cortical thickness and surface area variations in brain regions involved in “adaptive” or “top-down” modulation predominantly including fronto-parietal regions. Eventually, this study might contribute to a better biological understanding of this promising clinical tool for detecting the early development of schizophrenia [76].

Materials and methods

Study subjects

A sample of 22 right-handed, antipsychotic-naïve patients, fulfilling the pertinent diagnostic criteria of the paranoid subtype of schizophrenia (DSM-IV-R: 295.30) was consecutively recruited from the Department of Psychiatry and Psychotherapy in Cologne, Germany, between 2002 and 2006. A subset of these subjects has already been included in previous studies on BDII in schizophrenia spectrum disorders [51, 52, 69]. Subjects were excluded if: they (1) were aged < 18 or > 45 years, (2) were suffering from other relevant neurological or psychiatric diseases, (3) had a history of psychiatric symptoms or disease, (4) or other medical disorders potentially influencing neurocognitive function, (5) or had shown alcohol/substance abuse or dependence within 12 months prior to participation. The study was conducted in accordance with the Declaration of Helsinki and was approved by the ethics committees of the University of Cologne. All participants signed written informed consent.

Binocular depth inversion illusion (BDII) test and clinical assessments

All study subjects had normal stereoscopic vision [tested using the TNO test (Lameris, Utrecht, The Netherlands)] and reported no ophthalmological anomalies. A detailed

description of the BDII test can be found elsewhere [51, 56] and is only briefly summarized in the following. Two different sets of stereoscopic photographs were used as stimuli: 10 pictures of ordinary objects (e.g., chair, flower) and 9 frontal views of middle-age male human faces with a neutral expression, whereby half of the stimuli were presented in upside-down orientation. Each stimulus was presented twice via a mirror stereoscope, either as 3D normal (regular) or 3D inverted depiction (pseudoscopic, visual information for the right eye is presented to the left eye and vice versa) for no longer than 60 s in a random order. Prior to BDII testing, participants were instructed that the following stimuli would be either convex (3D normal) or concave (3D inverted). Participants were asked to describe their visual experience for each photograph with regard to overall impression and to selected parts of each object or face (e.g., depth of the nose), on a five-point rating scale ranging from ‘clearly concave’, ‘concave’, ‘flat/plane’, ‘convex’ to ‘clearly convex’. Each time, a maximum score of four was given for correct depth identification, whereas a completely inverted perception was assessed with zero points. To assess the degree of binocular depth inversion perception, we calculated an overall score (BDII total score): sum of all inverted object and human faces ratings divided by the maximum score possible. However, the BDII test allows computing additional sub-scores (BDII object score, BDII flower score, and BDII faces score). As the BDII faces score (sum of all inverted human faces ratings divided by the maximum faces score possible) was most affected in the previous studies [56, 69, 78], we decided to have a look at this score and its two sub-scores [BDII faces upside-down score (FUSD) and BDII faces right way up score (FRWU)], as well. All BDII scores range from zero (total BDII, i.e., ‘internally adjusted depth perception’) to one (no BDII, i.e., ‘unadjusted depth perception’) [51].

Structural MRI data acquisition

MRI data were acquired at the Department of Psychiatry and Psychotherapy, Cologne, Germany, on a 1.5 T scanner Philips Gyroscan NT Intera (Philips Eindhoven NL) with a standard birdcage head coil using a T1-FFE sequence with the following parameters: TR 30 ms, TE 4.5 ms, flip angle 30°, 120 slices, 256 × 256 matrix, field of view 256 × 256 mm, and slice spacing 3 mm. An experienced neuroradiologist reviewed all MRI brain scans; no gross abnormalities (e.g., tumor, space-occupying cystic lesion greater 3 mm, signs of bleeding, contusion, infarction, and major grey- or white-matter lesions) were found.

Image processing

Entire cortex analyses were computed with Freesurfer 6.0 [for detailed description of the method, see (<http://surfer>

r.nmr.mgh.harvard.edu/) [49] to explore the correlation between BDII performance and cortical thickness and surface area in the study sample [15, 23, 24]. Briefly, the stream consists of multiple stages such as removal of non-brain tissue using a hybrid watershed/surface deformation procedure [77]; affine registration with Talairach space specifically designed to be insensitive to abnormalities and to maximize the accuracy of the final segmentation; tissue classification and correction of the variation in intensity resulting from the B1 bias field [80]; tessellation of the grey-matter–white-matter boundary; automated topology correction, and surface deformation following intensity gradients to optimally place the gray/white and gray/cerebrospinal fluid borders at the location where the greatest shift in intensity defines the transition to the other tissue class [15]. After the automatic processing, the entire cortex of each patient was visually inspected and if necessary manually edited. After creation of cortical masks, the cerebral cortex has been parceled out into units based on gyral and sulcal structure, resulting in values for cortical thickness and surface area [18, 25]. Similar MRI data processing and statistical analyses steps were used in previous studies on psychiatric disorders [35, 39, 40].

MRI data processing and statistical analyses

Cortical surface modeling

In the first step, using a GLM approach provided by the Query Design Estimate Contrast (QDEC) interface of FreeSurfer, we performed a vertex-wise analysis across the entire study sample to explore the significant correlations between BDII performance [BDII total score, BDII faces score, BDII faces upside-down score (FUSD), and BDII faces right way up score (FRWU)] and cortical thickness and surface area variations. Age and gender were included as nuisance variables in these analyses. For statistical analysis, individual cortical thickness and surface area maps were registered to the fsaverage template included in FreeSurfer. Additional smoothing with full-width-half-max (FWHM) size of the Gaussian blurring kernel of 15 mm was applied on the statistical level [36, 70]. All of these analyses were performed on the right hemisphere and left hemisphere separately. Significant correlations between BDII scores and cortical parameters will be reported when their area exceeded 100 mm². The cluster size of 100 mm² was chosen in accordance with the ‘matched filter theorem’ [10, 11, 45] and has been already used in a previous structural MRI study on recent-onset schizophrenia patients [40].

Statistical analyses

In the second step, we extracted the cortical thickness and surface area values of the respective regions that exceeded

an area of 100 mm² from QDEC (or after Monte Carlo simulation and clustering) as implemented in FreeSurfer and put them into relation with BDII performance in the entire study sample. The correlations between BDII scores (dependent variable) and cortical thickness and surface area in the respective regions (explanatory variable) were explored using linear regression analysis. In the third step, to account for false positive findings within the identified regions, *p* values of the regression analyses were corrected using the classical Bonferroni correction. To this end, α was set to $p = 0.05/N$, where $N (= 16)$ equaled the number of correlations (classical Bonferroni correction). For this reason, the corrected threshold was set to $p = 0.003$ ($\alpha = 0.05/16$ tests [one study group \times two hemispheres \times two measurements \times four BDII tests]).

Monte Carlo simulation and clustering

We also tested the results from analytical step one against an empirical null distribution of maximum cluster size across 10,000 iterations using Z Monte Carlo simulations as implemented in FreeSurfer 6.0 [33, 34, 82]. Monte Carlo simulation was performed to identify significant contiguous clusters of vertex-wise morphological changes of cortical thickness and surface area correlated with BDII scores. An initial threshold of $p < 0.05$ (two-sided) for both the simulation step and the clustering step for the original data was chosen. The cluster-wise probability (CWP) resulting from the simulation and clustering is equivalent to the overall alpha significance level. This statistical approach (cluster-wise correction for multiple comparisons) has been described in prior publications [36, 38, 74, 75, 82]. Finally, we also extracted the cortical thickness and surface area values of the respective regions within the significant cluster and put them into relation with BDII performance in the entire study sample.

Results

Demographic details, psychopathological data, and BDII scores are shown in Table 1. In the first analytical step, we identified a total of 13 regions (5 in the left and 8 in the right hemisphere) with a relationship between cortical thickness and BDII performance, at a significance level of $p < 0.01$, varying in size between 111.35 and 656.10 mm² (Table 2). Furthermore, we identified a total of 11 regions (3 in the left hemisphere and 8 in the right hemisphere) with a relationship between surface area and BDII performance, at a significance level of $p < 0.01$, varying in size between 100.28 and 1198.44 mm² (Table 2).

In the second analytical step, we performed linear regression analyses in brain regions identified in step one

Table 1 Demographic data and clinical parameters

	Antipsychotic-naïve schizophrenia patients
Gender	
Male	11
Female	11
Education	
None	1
Modern secondary school-leaving certificate	3
Higher secondary school-leaving certificate	7
A-Level exam	9
Still at school	2
Professional training	
None	5
Apprenticeship	7
University	3
Still in professional training	7
Age (years)	
Median (min, 25th, 75th, max)	28 (18, 22, 37, 45)
PANSS scores [median (min, 25th, 75th, max)]	
Positive	23 (11, 20, 25, 30)
Negative	18 (10, 14, 24, 37)
General	44 (27, 37, 50, 68)
Total	88 (59, 71, 99, 134)
BDII scores [median (min, 25th, 75th, max)]	
Faces	0.39 (0.08, 0.31, 0.57, 0.97)
Total	0.43 (0.16, 0.33, 0.56, 0.90)

PANSS Positive and Negative Syndrome Scale, BDII binocular depth inversion illusion

and detected the following correlations between BDII performance and cortical thickness and surface area in the study sample: First, we found a significant positive correlation between BDII total scores and cortical thickness in the right postcentral gyrus [$F_{(1,20)} = 17.24$; $p = 0.0005$; $R^2 = 0.46$]. We also identified a significant positive correlation between BDII faces scores and cortical thickness in the right postcentral gyrus [$F_{(1,20)} = 18.36$; $p = 0.0004$; $R^2 = 0.47$], right pars triangularis of the inferior frontal gyrus (IFG) [$F_{(1,20)} = 15.02$; $p = 0.0009$; $R^2 = 0.42$], and left postcentral gyrus [$F_{(1,20)} = 6.44$; $p = 0.01$; $R^2 = 0.24$] (Fig. 1). Second, we found a significant positive correlation between BDII FRWU scores and cortical thickness in the left postcentral [$F_{(1,20)} = 16.28$; $p = 0.0006$; $R^2 = 0.44$] and middle temporal gyrus [$F_{(1,20)} = 14.59$; $p = 0.001$; $R^2 = 0.42$]. Third, we detected a significant negative correlation between BDII FUSD scores and cortical thickness in the left superior parietal gyrus [$F_{(1,20)} = 11.34$; $p = 0.003$; $R^2 = 0.36$], the left cuneus [$F_{(1,20)} = 7.41$; $p = 0.01$; $R^2 = 0.27$], and the left pericalcarine gyrus [$F_{(1,20)} = 1.62$; $p = 0.21$; $R^2 = 0.07$] (Fig. 2). We also identified a significant positive correlation between BDII FUSD scores and cortical thickness in the right postcentral gyrus [$F_{(1,20)} = 12.6$; $p = 0.002$; $R^2 = 0.38$]. Fourth, we

found a significant negative correlation between BDII total scores and surface area in the left superior parietal gyrus [$F_{(1,20)} = 8.48$; $p = 0.008$; $R^2 = 0.29$] and the right lateral occipital gyrus [$F_{(1,20)} = 2.61$; $p = 0.12$; $R^2 = 0.11$] (Fig. 3). There was also a significant positive correlation between BDII total scores and surface area in the right postcentral gyrus [$F_{(1,20)} = 14.77$; $p = 0.001$; $R^2 = 0.42$] (Fig. 3). However, the correlation between BDII total scores and surface area in the right lateral occipital gyrus did not reach statistical significance (Fig. 3). Fifth, we found a negative correlation between BDII faces scores and surface area in the left superior parietal gyrus [$F_{(1,20)} = 7.57$; $p = 0.01$; $R^2 = 0.27$] and the right lateral occipital gyrus [$F_{(1,20)} = 1.61$; $p = 0.21$; $R^2 = 0.07$]. We also found a positive correlation between BDII faces scores and surface area in the right postcentral gyrus [$F_{(1,20)} = 17.56$; $p = 0.0005$; $R^2 = 0.46$]. Sixth, we identified a negative correlation between BDII FRWU scores and surface area in the left lateral occipital gyrus [$F_{(1,20)} = 2.67$; $p = 0.11$; $R^2 = 0.11$]. Finally, we found a negative correlation between BDII FUSD scores and surface area in the left superior parietal gyrus [$F_{(1,20)} = 7.27$; $p = 0.01$; $R^2 = 0.26$], the right supramarginal gyrus [$F_{(1,20)} = 5.31$; $p = 0.03$; $R^2 = 0.2$], and the right lateral occipital gyrus

Table 2 Association between BDII performance and cortical measurements ($n=22$)

Cortical measurement	BDII score	Brain region	Area (mm ²)	CWP (p values)	Peak coordinates (Tal X, TalY, TalZ)	
Cortical thickness	BDII total score	Right postcentral gyrus (+)	111.35	–	51.1 – 14.7 38.2	
		BDII faces score	Left postcentral gyrus (+)	114.21	–	– 26.4 – 32.4 69.2
	BDII FRWU score	Right postcentral gyrus (+)	150.07	–	51.1 – 14.7 38.2	
		Right pars triangularis of inf. frontal Gr. (+)	163.71	–	43.3 31.8 – 1.1	
		Left postcentral gyrus (+)	659.10	–	– 62.7 – 20.3 – 14.8	
		Left middle temporal gyrus (+)	122.14	–	– 24.4 – 35.0 62.4	
Cortical area	BDII FUSD score	Right postcentral gyrus (+)	284.49*	0.007	51.8 – 13.8 33.4	
		Right middle temporal gyrus (+)	129.52*	0.007	47.6 – 58.5 0.6	
		Right superior parietal gyrus (+)	343.46*	0.007	30.8 – 35.8 44.1	
	BDII FRWU score	Right lateral occipital gyrus (+)	111.19*	0.007	22.6 – 95.4 12.2	
		Left superior parietal gyrus (–)	330.32	–	– 10.0 – 82.6 32.5	
		Left pericalcarine gyrus (–)	177.76	–	– 19.7 – 69.0 8.3	
		Right postcentral gyrus (+)	144.77	–	41.4 – 26.1 56.8	
		BDII total score	Left superior parietal gyrus (–)	362.0	–	– 37.1 – 50.1 58.6
		BDII faces score	Right lateral occipital gyrus (–)	797.98	–	28.3 – 95.6 – 4.2
			Right postcentral gyrus (+)	100.28	–	37.7 – 26.9 52.1
			Left superior parietal gyrus (–)	430.27	–	– 37.3 – 50.4 57.4
		BDII FRWU score	Right lateral occipital gyrus (–)	1198.44	–	27.3 – 97.3 – 4.5
			Right postcentral gyrus (+)	183.97	–	37.0 – 28.2 53.9
			Right lateral occipital gyrus (–)	541.63	–	32.2 – 89.7 – 3.1
			BDII FUSD score	Left superior parietal gyrus (–)	474.38	–
		BDII FRWU score	Right supramarginal gyrus (–)	207.39	–	36.6 – 34.1 19.3
			Right postcentral gyrus (+)	198.45	–	38.4 – 26.1 50.8
			Right lateral occipital gyrus (–)	169.89	–	22.1 – 98.3 – 4.3

Significant regions in both hemispheres with an area size exceeding 100 mm², p values from the vertex-wise comparison of mean cortical thickness and surface area and BDII performance ($p < 0.01$). Regions within a significant cluster that survived the Monte Carlo simulation ($p < 0.05$, CWP corr.) are marked with an asterisk (*)

FUSD BDII faces upside-down score, FRWU BDII faces right way up score

[$F_{(1,20)} = 0.61$; $p = 0.44$; $R^2 = 0.02$], as well as positive correlation between BDII FUSD scores and surface area in the right postcentral gyrus [$F_{(1,20)} = 19.14$; $p = 0.0003$; $R^2 = 0.489$]. In the third analytical step, p values of the regression analyses were corrected using the classical Bonferroni correction ($p < 0.003$). 10 of 20 correlations survived the Bonferroni correction for multiple testing.

Monte Carlo simulation and clustering

Cluster analysis via Monte Carlo simulation identified one cluster with a relationship between cortical thickness and BDII faces with a size of 2198.71 mm² at a significance level of $p < 0.05$ (Fig. 4). After extracting the cortical thickness values of neurobiologically relevant regions, we found a significant positive correlation between BDII FRWU scores and cortical thickness in the right superior parietal gyrus [$F_{(1,20)} = 15.96$; $p = 0.0007$; $R^2 = 0.44$], postcentral gyrus [$F_{(1,20)} = 11.21$; $p = 0.003$; $R^2 = 0.35$], supramarginal gyrus [$F_{(1,36)} = 16.39$; $p = 0.0006$; $R^2 = 0.45$], and precentral

gyrus [$F_{(1,20)} = 15.96$; $p = 0.0007$; $R^2 = 0.44$] (Fig. 4). However, there were no clusters with a relationship between BDII scores and surface area in schizophrenia patients that remained significant after the Monte Carlo simulation at a significance level of $p < 0.05$.

Discussion

This is the first structural neuroimaging study to specifically address cortical thickness and surface area variations correlated with disturbances in visual information processing using the BDII in antipsychotic-naïve first-episode schizophrenia patients. Three main findings emerged: (1) We found a significant correlation between BDII performance and cortical thickness changes in the inferior frontal gyrus, superior parietal gyrus, postcentral gyrus, and precentral gyrus, respectively. (2) BDII performance was significantly correlated with surface area in the superior parietal gyrus, supramarginal gyrus, and right postcentral gyrus.

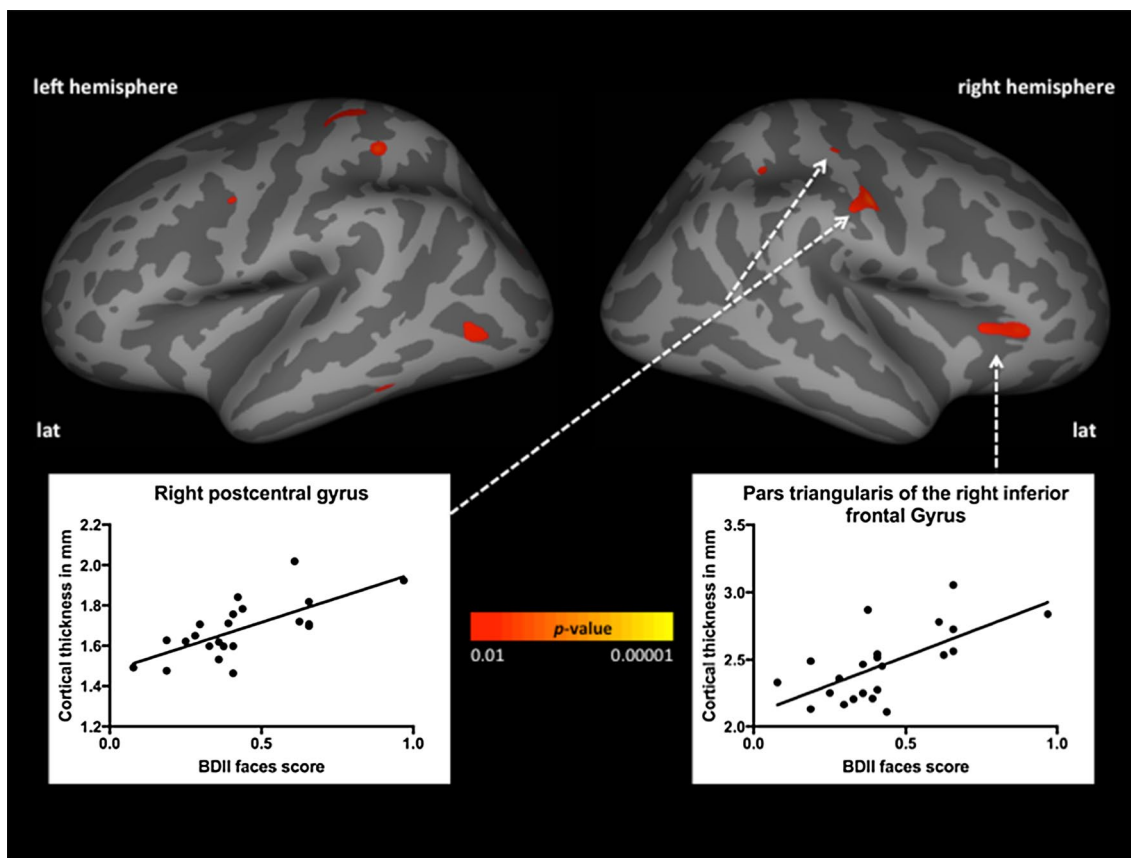


Fig. 1 Significant positive (red) associations between BDII faces scores and cortical thickness in the whole-study sample; co-varied for age and gender ($p < 0.01$, uncorrected). Scatter plots of linear regres-

sion analyses of cortical thickness and BDII faces scores in the right postcentral gyrus and pars triangularis of the inferior frontal gyrus

(3) Overall, cortical thickness and surface area differently contributed to BDII performance by means of their correlation directionality. We now discuss these findings in more detail and relate them to recent evidence on impaired BDII and aberrant visual information processing in schizophrenia spectrum disorders.

Cortical thickness

One major aim of the present structural MRI study was to expand the findings reported in earlier studies of our group [51, 52, 55, 56, 69] by presenting neural correlates of BDII in a sample of young, antipsychotic-naïve first-episode schizophrenia patients. In line with our predictions, our results showed that BDII performance was positively correlated with cortical thickness in the pars triangularis of the IFG, superior parietal gyrus, postcentral gyrus (somatosensory cortex), middle temporal gyrus, supramarginal gyrus, and precentral gyrus, respectively. These findings are relevant for a number of reasons: First, IFG is part of the mirror neuron system with a specific role in social cognition [43, 85]. Second, the superior parietal gyrus plays a

pivotal role in somatosensory and visuomotor integration [14] as well as processing of human emotional faces [28]. Third, the postcentral gyrus is part of the sensorimotor network (together with precentral and paracentral gyrus) and plays a crucial role in social cognition, including perception of facial expressions and emotions [57, 88]. Furthermore, the postcentral gyrus is the location of the primary somatosensory cortex that is involved in proprioception [7]. Fourth, the supramarginal gyrus together with angular gyrus composes the inferior parietale lobule (IPL) and this complex is responsible for processing of somatosensory and visual inputs from the brain. In addition, neurophysiological studies consistently reported that IPL is responsible for the immediate guidance of our bodily actions in space [29, 39, 46]. IPL and precuneus play critical role in visual and attention-related activities [90]. Remarkably, Wang et al. [87] found that there are primary connections between the first left and right subregions of the superior parietal gyrus and the postcentral gyrus, IPL, and inferior frontal gyrus via the superior longitudinal fasciculus suggesting an anatomical network responsible for visuomotor and observational processes. Our results strongly corroborate those presented

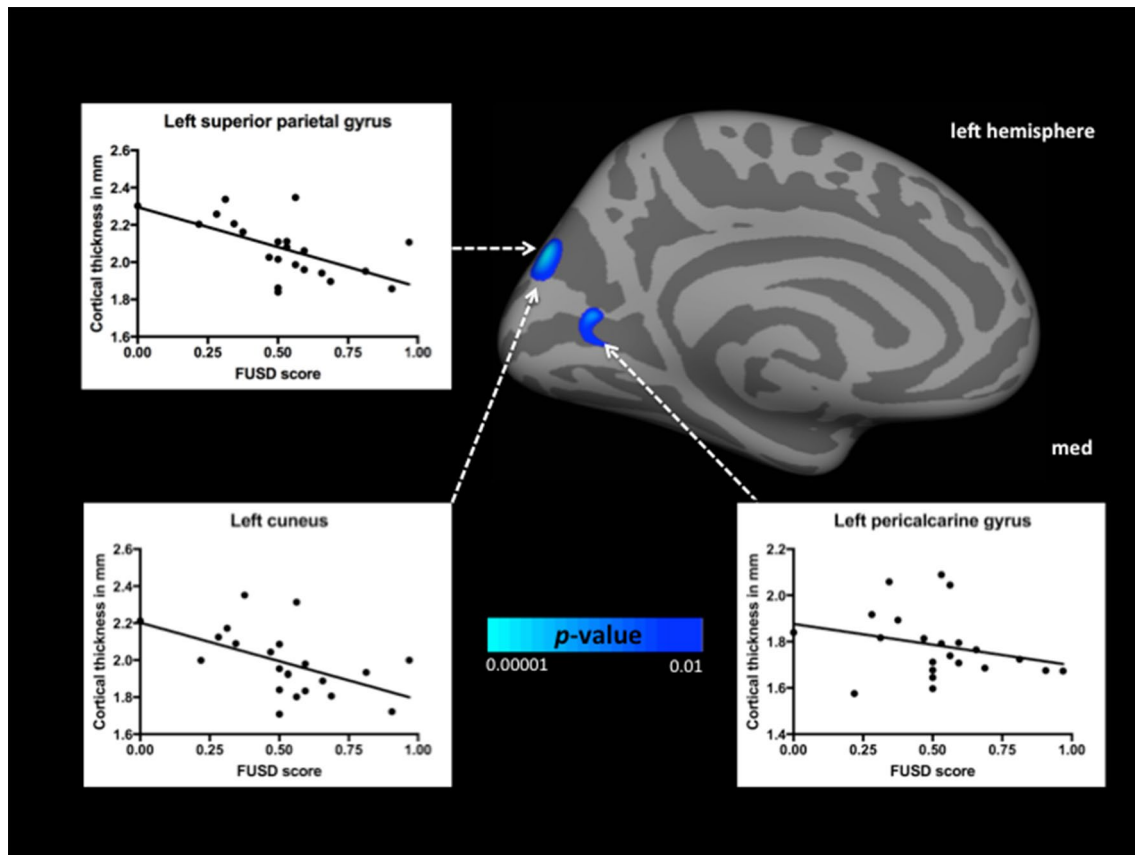


Fig. 2 Significant negative (blue) associations between BDII FUSD scores and cortical thickness in the whole-study sample; co-varied for age and gender ($p < 0.01$, uncorrected). Scatter plots of linear regres-

sion analyses of cortical thickness and BDII FUSD scores in the left superior parietal gyrus, left cuneus, and left pericalcarine gyrus

by Gupta et al. [32] who found that lower depth inversion illusion, i.e., a more veridical perception, was correlated with lower connectivity within the fronto-parietal network in UHR individuals. The authors concluded that lower connectivity within the fronto-parietal network and regions related to visual processing lead to aberrant modulation of sensory input [32]. A recent study conducted by Collin and colleagues [12] also supports our findings, because the authors found a disturbed grey-matter coupling between the supramarginal gyrus and postcentral gyrus in schizophrenia. Altogether, these results are largely consistent with the literature on brain areas primarily involved in “adaptive” or “top-down” modulation and stimulus processing [6, 19, 31] and might explain disturbed facial and visuo-spatial recognition, which can result in the inability to adjust depth perception of human faces. The above-mentioned regions are also in line with MRI studies on schizophrenia that showed grey-matter alterations in frontal, temporal, and parietal structures [44, 62, 66]. Finally, cortical thickness alterations in the fronto-parietal and occipital regions might represent a neurobiological continuum of BDII-related anatomical patterns across schizophrenia spectrum disorders.

On further inspection, we also found a negative correlation between BDII FUSD scores and cortical thickness changes in the left superior parietal gyrus, the left cuneus, and the left pericalcarine gyrus. These findings are also neurobiologically relevant for a number of reasons: First, the superior parietal gyrus is involved not only in visuo-spatial and attentional processing of the space surrounding one’s body, but also in working memory [50, 61] and processing, as well as recognizing of human emotional faces [1, 2, 28]. This region contains a mosaic of functionally and structurally distinct subregions, which serve different physiological functions [87]. In conjunction with findings from recent studies, we speculate that different component subregions of the superior parietal gyrus might explain the coexisting positive and negative correlations between BDII performance and cortical thickness in this area [71, 72]. Second, the cuneus belongs to the occipital lobe. Although there have been only few MRI studies that found neuroanatomical alterations of the occipital lobe in schizophrenia [3, 16, 92], deficits in the early visual processing have been repeatedly reported [21, 48] suggesting its specific role in the pathophysiology of schizophrenia. Third, the pericalcarine

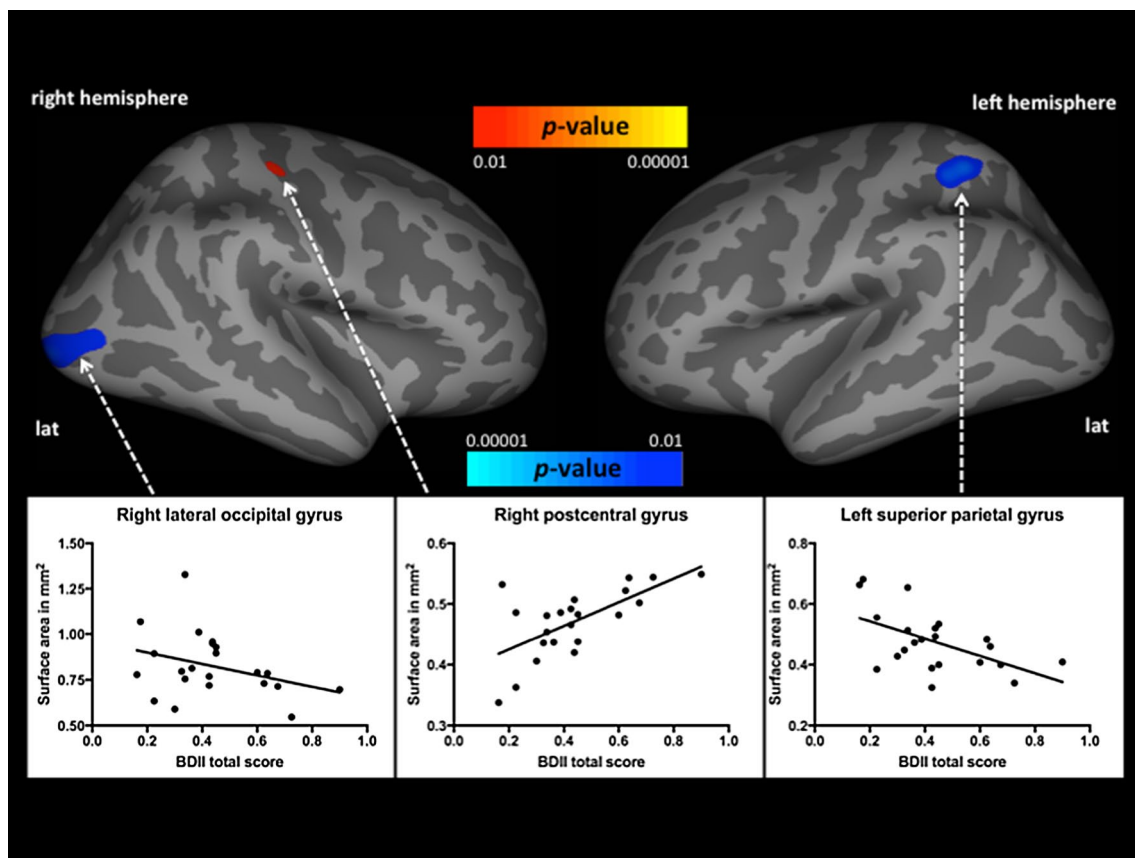


Fig. 3 Significant positive (red) and negative (blue) associations between BDII total scores and surface area in the whole-study sample; co-varied for age and gender ($p < 0.01$, uncorrected). Scatter

plots of linear regression analyses of cortical thickness and BDII total scores in the right lateral occipital, postcentral, and left superior parietal gyrus

cortex encompasses the primary visual cortex (V1) and the precuneus. On one hand, V1 is the entry point of visual information into cortical circuits. On the other hand, the precuneus plays a crucial role in visuo-spatial tasks [13], integration of stimuli, and experience of agency [5, 17]. These findings are remarkable, because they correspond well with the requirements of BDII and are consistent with those presented by Dima et al. [19], who found significantly increased effective connectivity between lateral occipital cortex and V1 when schizophrenia patients were presented with 3D inverted faces. Furthermore, our observations are once again in accordance with Gupta et al. [32], who found a negative correlation between weaker connectivity from IFG to lingual gyrus (part of pericalcarine cortex) and veridical perception in UHR individuals. Furthermore, these regions correlate well with the literature on schizophrenia. In particular, a recent meta-analysis of emotional processing studies found a hyperactivation of the parietal lobule, temporal lobes, and cuneus in schizophrenia patients [83]. On one hand, we found a negative correlation between cortical thickness in parieto-occipital regions and BDII performance. Cortical thickness alterations in these regions might also be

attributed, in part, to connectivity changes within this network as previously reported [32]. On the other hand, there is an increased connectivity or hyper-activity in parieto-occipital networks responsible for facial recognition and visual processing in schizophrenia [83]. Findings from other studies together with our results suggest a disordered modulatory top-down control in schizophrenia patients exhibiting higher BDII scores. We hypothesize that these findings complement each other and reflect a neuroanatomical maladaptive abnormality in schizophrenia patients exhibiting impairment of visual information processing as assessed with BDII. However, the comparison of our results with the previous studies is not trivial, because we did not investigate functional connectivity parameters and found only correlation between BDII performance and cortical thickness. Given the lack of a control group, we cannot drive any strong conclusions on whether BDII performance is correlated with increase or decrease of cortical thickness.

Interestingly, BDII was more pronounced with regard to FRWU than to FUSD stimuli, indicating that higher familiarity strengthens “adaptive” or “top-down” processing, even if the balance between “top-down” and “bottom-up”

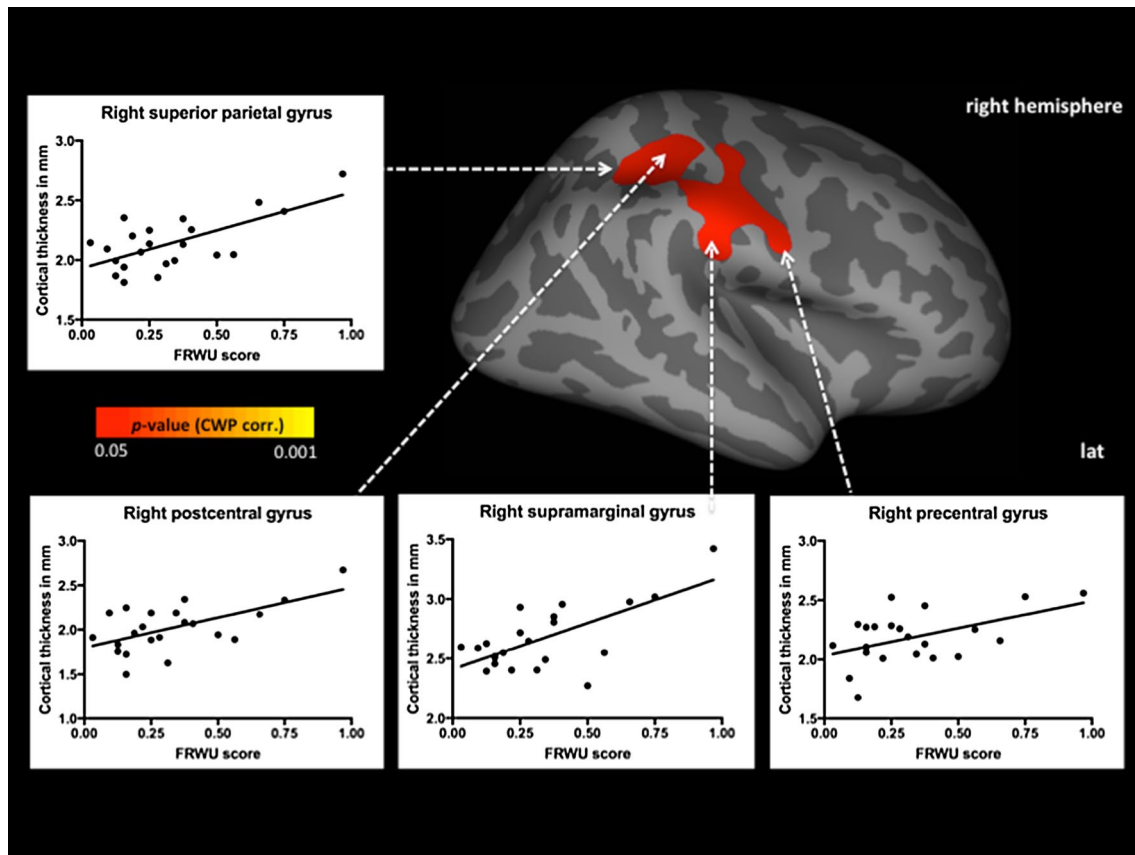


Fig. 4 Significant positive (red) associations between BDII FRWU scores and cortical thickness in the whole-study sample; co-varied for age and gender ($p < 0.05$, CWP corrected). Scatter plots of linear

regression analyses of cortical thickness and BDII FRWU scores in the right superior parietal, postcentral, supramarginal, and precentral gyrus

processes is disturbed. All stimuli consisted of two photographs, and, therefore, comprise visual cues that favor the illusion, such as shading and realistic features in faces and objects. However, by turning the faces upside-down, realistic features and shading play a less important role. Therefore, it might be speculated that the different correlations observed for FUSD, FRWU, and BDII faces scores with cortical thickness alterations are influenced by the different visual cues used for depth perception. However, to disentangle how the different cues interact and how they affect brain activity, further imaging studies are needed, using different kinds of stimuli.

There are other cues, beside binocular disparity, that favor veridical physical depth perception, such as vergence angle, lens accommodation, and motion parallax, while painted cues, such as perspective and foreshortening as well as realistic features and shading, favor depth inversion [20]. It has been suggested that, when the visual system receives strong conflicting signals for identifying depth, such as binocular disparity and linear-perspective cues, it might, additionally, rely on vergence angle, possibly combined with cues from accommodation and the resulting blur, and maybe also on

the binocular disparity scaled by the retinal size of the object [20]. These cues compete with conceptual expectations (“top–down” factors). The balance between these conflicting inputs determines, whether the veridical physical depth perception or the illusion is more predominant. It has been suggested that in schizophrenia patients, the “top–down” processing is attenuated, resulting in a more veridical depth perception [19, 51, 56, 78]. Keane et al. [47] found that schizophrenia patients experience fewer DIIs with a variety of object types and viewing conditions. The authors [47] suggested that schizophrenia patients have, in general, a reduced tendency to construe any type of object as convex, while processing of face, stereoscopic, or texture information is not disturbed. However, so far, nothing is known about the underlying brain activity towards the different stimuli. Although Gupta et al. [32] used two different mask stimuli—with and without texture—connectivity analyses were only conducted using the texture mask condition, as the difference between UHR individuals and healthy controls in depth inversion illusion susceptibility was more pronounced in this testing condition. Thus, future neuroimaging studies should try to analyze how different visual cues that favor

veridical depth perception or illusion influence brain activity in healthy subjects and schizophrenia patients.

Surface area

We also found correlations between surface area changes and BDII performance in the left superior parietal gyrus, the right postcentral gyrus, and the right lateral occipital gyrus. Although the correlation between BDII total scores and surface area in the right lateral occipital gyrus did not reach statistical significance, these three brain regions are useful in building a cumulative understanding of BDII in schizophrenia. In line with the previous studies on BDII in schizophrenia spectrum disorders, surface area changes in the above-mentioned three regions and cortical thickness changes in the pars triangularis of IFG and supramarginal gyrus complement each other very well, and thus endorse the importance of brain regions responsible for processing of visuo-spatial stimuli and cognitive control in the pathophysiology of the BDII in schizophrenia. These regions corroborate the previous studies that postulated dysfunction of the magnocellular pathway in the early visual processing of schizophrenia patients [8, 53, 58, 59]. What become evident are both different and overlapping patterns of cortical alterations in terms of surface area and cortical thickness, and parameters differentially influenced by evolutionary, genetic, and cellular processes [67, 68, 86]. On one hand, cortical thickness changes reflect dynamic synaptic reorganization according to environmental influences [63, 81, 86, 91]; and hence, it might be considered as an indicator of adverse events during the adulthood [81]. On the other hand, cortical area changes are stable, because they are related to changes in cortical gyrification during the early phases of brain development [41, 86]. Therefore, our findings might reflect a gene-environment interaction in the pathophysiology of impaired BDII in schizophrenia patients. Overall, our findings suggest that poorer BDII performance might be primarily correlated with alterations of cortical surface parameters suggesting a dysbalance between fronto-parietal and occipital regions.

Our study revealed that BDII-related cortical thickness and surface area alterations are regionally circumscribed involving mainly schizophrenia vulnerable regions rather than evenly distributed throughout the entire brain. Furthermore, the negative and positive correlations between cortical thickness and surface area changes and BDII performance in our study indicate that there is no reciprocal relationship between neural structure and impairment in visual information processing in first-episode schizophrenia patients. Thus, the directionality of our present findings might reflect structural change, i.e., hypertrophy or atrophy as found in previous studies on schizophrenia [30, 42]. Furthermore, one might speculate that the different directionalities of the

identified correlation illustrate both aberrant visual processing and some compensatory behavioral strategies and brain mechanisms in schizophrenia. Taken together, we observed brain alterations in some areas previously identified by functional connectivity studies [9, 26, 79], presumably underlying BDII performance in schizophrenia. However, cortical thickness or area changes are not synonymous with functional status [87], and the above-mentioned dissociation serves as a reminder for the complex neurobiological underpinnings in schizophrenia.

Strengths and limitations

Strengths of this study include the use of the latest FreeSurfer version 6.0, the rigorous use of multiple comparisons corrections, and the antipsychotic-naïve first-episode study population. By examining antipsychotic-naïve first-episode schizophrenia patients, we were able to exclude the possibility that confounding factors (long-term disease-specific processes, chronicity, comorbidities, and antipsychotic medication) [4] might have influenced the findings. To the best of our knowledge, this is the first structural neuroimaging study to investigate two distinct cortical parameters correlated with BDII performance in antipsychotic-naïve first-episode schizophrenia patients. Nevertheless, there are several limitations that need to be considered when interpreting and discussing our findings. The sample size, the cross-sectional design, and the lack of the control group may be seen as limitations of our study. Given that we used a correlational approach, it is not possible to conclude on causal mechanisms underlying BDII impairments in the first-episode schizophrenia patients. Cortical thickness and surface area alterations probably account only for small part of the variations underlying aberrant BDII performance in schizophrenia. With respect to sample size, however, it is noteworthy that there is only one neuroimaging study that investigated neural underpinning of BDII in schizophrenia [19]. Another limitation of this study is related to the use of 1.5 T MRI in our present study [35]. MRI at 1.5 T is less sensitive to signal changes than MRI at 3 T [65] and might have led to spatial inaccuracies. Given that we found cortical thickness and area changes in brain regions responsible for somatosensory functions and visuo-spatial processing, which corroborate the previous volumetric MRI studies in schizophrenia, our results are neurobiologically plausible [35]. Furthermore, given the availability of only two MRI studies on BDII in schizophrenia spectrum disorders that used different methods of data acquisition and analysis, it is premature to draw definitive conclusions on cortical alterations underlying this specific test [35]. Another issue worth commenting is that the majority of the brain regions identified in the analytical step one did not survive cluster-wise correction

for multiple comparisons (Monte Carlo simulation). This is interesting, since the previous MRI studies with similar number of subjects with psychotic disorders reported results corrected for multiple comparisons after the Monte Carlo simulation [35, 36, 40]. Although cluster-wise thresholding has been widely recognized as the most popular threshold method among the correction methods used in modern neuroimaging [27, 89], cluster-extent-based thresholding has low spatial specificity when clusters are large (for detailed information, see Woo et al. [89]). For the present study, it means that although we only identified two large clusters, these clusters contain a number of neurobiologically relevant regions (see Fig. 2) and these are true positive BDII-relevant areas. Still, we do not consider the other results as being false positive for two reasons: first, the specific purpose of this study was to better understand the cortex variations underlying BDII performance in schizophrenia. Since there is no previous study that used Freesurfer to answer this specific question, the cost of a false negative, when using Monte Carlo simulation, could be that we have missed out important BDII-related regionally confined cortex changes [37]. Therefore, we consider false negatives as being very costly under these conditions [37]. Second, after extracting the cortical thickness and surface area vertex values, linear regression analyses produced statistically significant results. These results survived classical Bonferroni correction, which is a very widely applicable, but also a very conservative statistical approach that might increase the risk for type 2 error and miss to detect meaningful results [37, 60]. Nonetheless, we suggest that reporting and discussing uncorrected results are very valuable in this particular case [37]. In spite of all the limitations, the promising data reflecting cortical signature of impaired BDII in schizophrenia might lead to development of a valid tool for the early diagnosis of psychotic disorders and schizophrenia in particular.

Conclusion

Our results lead to the postulate that there is a structural imbalance between fronto-parietal and occipital regions in the pathophysiology of impaired BDII performance in the first-episode schizophrenia. This study is broadly consistent with the aberrant “top–down” information processing in schizophrenia. In the future, larger patient population studies will have to be examined using multimodal neuroimaging methods to define the advantages of combining BDII with MRI. This combination could provide a deeper understanding of the effects of different visual cues on BDII, the interplay of “bottom–up” and “top–down” processes, and may lead to important insights

on mechanisms of system-level dysfunction in the first-episode schizophrenia.

Acknowledgements We thank Kristina Gawlik for technical support. We are grateful to all the participants and their families for their time and interest in this study.

Funding The authors have declared that there is no funding of this study.

Compliance with ethical standards

Conflict of interest The authors have declared that there are no conflicts of interest in relation to the subject of this study.

Ethical standards This study has been approved by the appropriate ethics committee and has, therefore, been performed in accordance with the ethical standards laid down in the 1964 Declaration of Helsinki and its later amendments.

References

1. Adolphs R (2002) Neural systems for recognizing emotion. *Curr Opin Neurobiol* 12:169–177
2. Adolphs R (2002) Recognizing emotion from facial expressions: psychological and neurological mechanisms. *Behav Cogn Neurosci Rev* 1:21–62
3. Andreasen NC, Flashman L, Flaum M, Arndt S, Swayze V 2nd, O’Leary DS, Ehrhardt JC, Yuh WT (1994) Regional brain abnormalities in schizophrenia measured with magnetic resonance imaging. *JAMA* 272:1763–1769
4. Bernard JA, Orr JM, Mittal VA (2017) Cerebello-thalamo-cortical networks predict positive symptom progression in individuals at ultra-high risk for psychosis. *NeuroImage Clin* 14:622–628
5. Binder J (1997) Functional magnetic resonance imaging. Language mapping. *Neurosurg Clin N Am* 8:383–392
6. Bridge H, Parker AJ (2007) Topographical representation of binocular depth in the human visual cortex using fMRI. *J Vis* 7(14):15.1–15.14. <https://doi.org/10.1167/7.14.15>
7. Buchy L, Barbato M, Makowski C, Bray S, MacMaster FP, Deighton S, Addington J (2017) Mapping structural covariance networks of facial emotion recognition in early psychosis: a pilot study. *Schizophr Res* 189:146–152. <https://doi.org/10.1016/j.schres.2017.01.054>
8. Calderone DJ, Hoptman MJ, Martinez A, Nair-Collins S, Mauro CJ, Bar M, Javitt DC, Butler PD (2013) Contributions of low and high spatial frequency processing to impaired object recognition circuitry in schizophrenia. *Cereb Cortex* 23:1849–1858
9. Cao H, Dixon L, Meyer-Lindenberg A, Tost H (2016) Functional connectivity measures as schizophrenia intermediate phenotypes: advances, limitations, and future directions. *Curr Opin Neurobiol* 36:7–14
10. Chung MK, Robbins SM, Dalton KM, Davidson RJ, Alexander AL, Evans AC (2005) Cortical thickness analysis in autism with heat kernel smoothing. *NeuroImage* 25:1256–1265
11. Chung MK, Worsley KJ, Robbins S, Paus T, Taylor J, Giedd JN, Rapoport JL, Evans AC (2003) Deformation-based surface morphometry applied to gray matter deformation. *NeuroImage* 18:198–213
12. Collin G, de Reus MA, Cahn W, Hulshoff Pol HE, Kahn RS, van den Heuvel MP (2013) Disturbed grey matter coupling in schizophrenia. *Eur Neuropsychopharmacol* 23:46–54

13. Corbetta M, Miezin FM, Shulman GL, Petersen SE (1993) A pet study of visuospatial attention. *J Neurosci* 13:1202–1226
14. Culham JC, Valyear KF (2006) Human parietal cortex in action. *Curr Opin Neurobiol* 16:205–212
15. Dale AM, Fischl B, Sereno MI (1999) Cortical surface-based analysis. I. Segmentation and surface reconstruction. *NeuroImage* 9:179–194
16. Davatzikos C, Shen D, Gur RC, Wu X, Liu D, Fan Y, Hughett P, Turetsky BI, Gur RE (2005) Whole-brain morphometric study of schizophrenia revealing a spatially complex set of focal abnormalities. *Arch Gen Psychiatry* 62:1218–1227
17. Dean K, Fearon P, Morgan K, Hutchinson G, Orr K, Chitnis X, Suckling J, Mallet R, Leff J, Jones PB, Murray RM, Dazzan P (2006) Grey matter correlates of minor physical anomalies in the aetiological first-episode psychosis study. *Br J Psychiatry* 189:221–228
18. Desikan RS, Segonne F, Fischl B, Quinn BT, Dickerson BC, Blacker D, Buckner RL, Dale AM, Maguire RP, Hyman BT, Albert MS, Killiany RJ (2006) An automated labeling system for subdividing the human cerebral cortex on mri scans into gyral based regions of interest. *NeuroImage* 31:968–980
19. Dima D, Roiser JP, Dietrich DE, Bonnemann C, Lanfermann H, Emrich HM, Dillo W (2009) Understanding why patients with schizophrenia do not perceive the hollow-mask illusion using dynamic causal modelling. *Neuroimage* 46:1180–1186
20. Dobias JJ, Papanthomas TV (2013) Recovering 3-D shape: roles of absolute and relative disparity, retinal size, and viewing distance as studied with reverse-perspective stimuli. *Perception* 42:430–446
21. Doniger GM, Foxe JJ, Murray MM, Higgins BA, Javitt DC (2002) Impaired visual object recognition and dorsal/ventral stream interaction in schizophrenia. *Arch Gen Psychiatry* 59:1011–1020
22. Emrich HM, Weber MM, Wendl A, Zihl J, Von Meyer L, Hanisch W (1991) Reduced binocular depth inversion as an indicator of cannabis-induced censorship impairment. *Pharmacol Biochem Behav* 40:689–690
23. Fischl B, Dale AM (2000) Measuring the thickness of the human cerebral cortex from magnetic resonance images. *Proc Natl Acad Sci USA* 97:11050–11055
24. Fischl B, Sereno MI, Dale AM (1999) Cortical surface-based analysis. II: inflation, flattening, and a surface-based coordinate system. *NeuroImage* 9:195–207
25. Fischl B, van der Kouwe A, Destrieux C, Halgren E, Segonne F, Salat DH, Busa E, Seidman LJ, Goldstein J, Kennedy D, Caviness V, Makris N, Rosen B, Dale AM (2004) Automatically parcellating the human cerebral cortex. *Cereb Cortex* 14:11–22
26. Fitzsimmons J, Kubicki M, Shenton ME (2013) Review of functional and anatomical brain connectivity findings in schizophrenia. *Curr Opin Psychiatry* 26(2):172–187. <https://doi.org/10.1097/YCO.0b013e32835d9e6a>
27. Friston KJ, Worsley KJ, Frackowiak RS, Mazziotta JC, Evans AC (1994) Assessing the significance of focal activations using their spatial extent. *Hum Brain Mapp* 1:210–220
28. Fusar-Poli P, Bhattacharyya S, Allen P, Crippa JA, Borgwardt S, Martin-Santos R, Seal M, O'Carroll C, Atakan Z, Zuardi AW, McGuire P (2010) Effect of image analysis software on neuro-functional activation during processing of emotional human faces. *J Clin Neurosci* 17:311–314
29. Gharabaghi A, Fruhmann Berger M, Tatagiba M, Karnath HO (2006) The role of the right superior temporal gyrus in visual search-insights from intraoperative electrical stimulation. *Neuropsychologia* 44:2578–2581
30. Gong Q, Lui S, Sweeney JA (2016) A selective review of cerebral abnormalities in patients with first-episode schizophrenia before and after treatment. *Am J Psychiatry* 173(3):232–243
31. Gregory RL (1998) *Eye and brain. The psychology of seeing.* Oxford University Press, Oxford
32. Gupta T, Silverstein SM, Bernard JA, Keane BP, Papanthomas TV, Pelletier-Baldelli A, Dean DJ, Newberry RE, Ristanovic I, Mittal VA (2016) Disruptions in neural connectivity associated with reduced susceptibility to a depth inversion illusion in youth at ultra high risk for psychosis. *NeuroImage Clin* 12:681–690
33. Hagler DJ Jr, Saygin AP, Sereno MI (2006) Smoothing and cluster thresholding for cortical surface-based group analysis of fMRI data. *NeuroImage* 33:1093–1103
34. Hayasaka S, Nichols TE (2003) Validating cluster size inference: random field and permutation methods. *NeuroImage* 20:2343–2356
35. Hirjak D, Huber M, Kirchler E, Kubera KM, Karner M, Sambataro F, Freudenmann RW, Wolf RC (2017) Cortical features of distinct developmental trajectories in patients with delusional infestation. *Progress Neuro Psychopharmacol Biol Psychiatry* 76:72–79
36. Hirjak D, Kubera KM, Wolf RC, Thomann AK, Hell SK, Seidl U, Thomann PA (2015) Local brain gyrification as a marker of neurological soft signs in schizophrenia. *Behav Brain Res* 292:19–25
37. Hirjak D, Thomann PA, Wolf RC, Kubera KM, Goch C, Hering J, Maier-Hein KH (2017) White matter microstructure variations contribute to neurological soft signs in healthy adults. *Hum Brain Mapp* 38:3552–3565
38. Hirjak D, Wolf RC, Kubera KM, Stieltjes B, Thomann PA (2016) Multiparametric mapping of neurological soft signs in healthy adults. *Brain Struct Funct* 221:1209–1221
39. Hirjak D, Wolf RC, Pfeifer B, Kubera KM, Thomann AK, Seidl U, Maier-Hein KH, Schroder J, Thomann PA (2017) Cortical signature of clock drawing performance in alzheimer's disease and mild cognitive impairment. *J Psychiatr Res* 90:133–142
40. Hirjak D, Wolf RC, Stieltjes B, Hauser T, Seidl U, Schroder J, Thomann PA (2014) Cortical signature of neurological soft signs in recent onset schizophrenia. *Brain Topogr* 27:296–306
41. Hogstrom LJ, Westlye LT, Walhovd KB, Fjell AM (2013) The structure of the cerebral cortex across adult life: age-related patterns of surface area, thickness, and gyrification. *Cereb Cortex* 23:2521–2530
42. Knöchel C, Reuter J, Reinke B, Stäblein M, Marbach K, Feddern R, Kuhlmann K, Alves G, Prvulovic D, Wenzler S, Linden DEJ, Oertel-Knöchel V (2016) Cortical thinning in bipolar disorder and schizophrenia. *Schizophr Res* 172(1–3):78–85
43. Iacoboni M, Molnar-Szakacs I, Gallese V, Buccino G, Mazziotta JC, Rizzolatti G (2005) Grasping the intentions of others with one's own mirror neuron system. *PLoS Biol* 3:e79
44. Janssen J, Aleman-Gomez Y, Schnack H, Balaban E, Pina-Camacho L, Alfaro-Almagro F, Castro-Fornieles J, Otero S, Baeza I, Moreno D, Bargallo N, Parellada M, Arango C, Desco M (2014) Cortical morphology of adolescents with bipolar disorder and with schizophrenia. *Schizophr Res* 158:91–99
45. Jung WH, Kim JS, Jang JH, Choi JS, Jung MH, Park JY, Han JY, Choi CH, Kang DH, Chung CK, Kwon JS (2011) Cortical thickness reduction in individuals at ultra-high-risk for psychosis. *Schizophr Bull* 37:839–849
46. Karnath HO (2001) New insights into the functions of the superior temporal cortex. *Nat Rev Neurosci* 2:568–576
47. Keane BP, Silverstein SM, Wang Y, Papanthomas TV (2013) Reduced depth inversion illusions in schizophrenia are state-specific and occur for multiple object types and viewing conditions. *J Abnormal Psychol* 122:506–512
48. Keri S, Janka Z (2004) Critical evaluation of cognitive dysfunctions as endophenotypes of schizophrenia. *Acta Psychiatr Scand* 110:83–91
49. Khan AR, Wang L, Beg MF (2008) Freesurfer-initiated fully-automated subcortical brain segmentation in mri using large deformation diffeomorphic metric mapping. *NeuroImage* 41:735–746

50. Koenigs M, Barbey AK, Postle BR, Grafman J (2009) Superior parietal cortex is critical for the manipulation of information in working memory. *J Neurosci* 29:14980–14986
51. Koethe D, Gerth CW, Neatby MA, Haensel A, Thies M, Schneider U, Emrich HM, Klosterkötter J, Schultze-Lutter F, Leweke FM (2006) Disturbances of visual information processing in early states of psychosis and experimental delta-9-tetrahydrocannabinol altered states of consciousness. *Schizophr Res* 88:142–150
52. Koethe D, Kranaster L, Hoyer C, Gross S, Neatby MA, Schultze-Lutter F, Ruhrmann S, Klosterkötter J, Hellmich M, Leweke FM (2009) Binocular depth inversion as a paradigm of reduced visual information processing in prodromal state, antipsychotic-naïve and treated schizophrenia. *Eur Arch Psychiatry Clin Neurosci* 259:195
53. Lee JS, Park G, Song MJ, Choi KH, Lee SH (2016) Early visual processing for low spatial frequency fearful face is correlated with cortical volume in patients with schizophrenia. *Neuropsychiatr Dis Treatm* 12:1–14
54. Leweke FM, Giuffrida A, Wurster U, Emrich HM, Piomelli D (1999) Elevated endogenous cannabinoids in schizophrenia. *Neuroreport* 10:1665–1669
55. Leweke FM, Schneider U, Radwan M, Schmidt E, Emrich HM (2000) Different effects of nabilone and cannabidiol on binocular depth inversion in man. *Pharmacol Biochem Behav* 66:175–181
56. Leweke FM, Schneider U, Thies M, Münte TF, Emrich HM (1999) Effects of synthetic δ 9-tetrahydrocannabinol on binocular depth inversion of natural and artificial objects in man. *Psychopharmacology* 142:230–235
57. Liu Y, Zhang Y, Lv L, Wu R, Zhao J, Guo W (2017) Abnormal neural activity as a potential biomarker for drug-naïve first-episode adolescent-onset schizophrenia with coherence regional homogeneity and support vector machine analyses. *Schizophr Res*
58. Martinez A, Hillyard SA, Bickel S, Dias EC, Butler PD, Javitt DC (2012) Consequences of magnocellular dysfunction on processing attended information in schizophrenia. *Cereb Cortex* 22:1282–1293
59. Martinez A, Hillyard SA, Dias EC, Hagler DJ Jr, Butler PD, Guilfoyle DN, Jalbrzikowski M, Silipo G, Javitt DC (2008) Magnocellular pathway impairment in schizophrenia: evidence from functional magnetic resonance imaging. *J Neurosci* 28:7492–7500
60. McDonald JH (2015) Handbook of biological statistics. Sparky House Publishing, Baltimore
61. Nachev P, Husain M (2006) Disorders of visual attention and the posterior parietal cortex. *Cortex* 42:766–773
62. Nenadic I, Maitra R, Langbein K, Dietzek M, Lorenz C, Smesny S, Reichenbach JR, Sauer H, Gaser C (2015) Brain structure in schizophrenia vs. psychotic bipolar I disorder: a VBM study. *Schizophr Res* 165:212–219
63. Oostermeijer S, Whittle S, Suo C, Allen NB, Simmons JG, Vijayakumar N, van de Ven PM, Jansen LM, Yucel M, Popma A (2016) Trajectories of adolescent conduct problems in relation to cortical thickness development: a longitudinal MRI study. *Transl Psychiatry* 6:e841
64. Palaniyappan L, Liddle PF (2012) Differential effects of surface area, gyrification and cortical thickness on voxel based morphometric deficits in schizophrenia. *NeuroImage* 60:693–699
65. Phal PM, Usmanov A, Nesbit GM, Anderson JC, Spencer D, Wang P, Helwig JA, Roberts C, Hamilton BE (2008) Qualitative comparison of 3-t and 1.5-t mri in the evaluation of epilepsy. *Am J Roentgenol* 191:890–895
66. Pina-Camacho L, Garcia-Prieto J, Parellada M, Castro-Fornieles J, Gonzalez-Pinto AM, Bombin I, Graell M, Paya B, Rapado-Castro M, Janssen J, Baeza I, Del Pozo F, Descio M, Arango C (2015) Predictors of schizophrenia spectrum disorders in early-onset first episodes of psychosis: a support vector machine model. *Eur Child Adolesc Psychiatry* 24:427–440
67. Rakic P (1995) The development of the frontal lobe. A view from the rear of the brain. *Adv Neurol* 66:1–6 (**discussion 6–8**)
68. Rakic P (1995) Radial versus tangential migration of neuronal clones in the developing cerebral cortex. *Proc Natl Acad Sci USA* 92:11323–11327
69. Reuter AR, Bumb JM, Mueller JK, Rohleder C, Pahlisch F, Hanke F, Arens E, Leweke FM, Koethe D, Schwarz E (2017) Association of anandamide with altered binocular depth inversion illusion in schizophrenia. *World J Biol Psychiatry* 18:483–488
70. Schaer M, Ottet MC, Scariati E, Dukes D, Franchini M, Eliez S, Glaser B (2013) Decreased frontal gyrification correlates with altered connectivity in children with autism. *Front Hum Neurosci* 7:750
71. Scheperjans F, Grefkes C, Palomero-Gallagher N, Schleicher A, Zilles K (2005) Subdivisions of human parietal area 5 revealed by quantitative receptor autoradiography: a parietal region between motor, somatosensory, and cingulate cortical areas. *NeuroImage* 25:975–992
72. Scheperjans F, Palomero-Gallagher N, Grefkes C, Schleicher A, Zilles K (2005) Transmitter receptors reveal segregation of cortical areas in the human superior parietal cortex: relations to visual and somatosensory regions. *NeuroImage* 28:362–379
73. Schneider U, Borsutzky M, Seifert J, Leweke FM, Huber TJ, Rollnik JD, Emrich HM (2002) Reduced binocular depth inversion in schizophrenic patients. *Schizophr Res* 53:101–108
74. Schultz CC, Koch K, Wagner G, Roebel M, Schachtzabel C, Gaser C, Nenadic I, Reichenbach JR, Sauer H, Schlosser RG (2010) Reduced cortical thickness in first episode schizophrenia. *Schizophr Res* 116:204–209
75. Schultz CC, Nenadic I, Koch K, Wagner G, Roebel M, Schachtzabel C, Muhleisen TW, Nothen MM, Cichon S, Deufel T, Kiehn-topf M, Rietschel M, Reichenbach JR, Sauer H, Schlosser RG (2011) Reduced cortical thickness is associated with the glutamatergic regulatory gene risk variant *daoa arg30lys* in schizophrenia. *Neuropsychopharmacology* 36:1747–1753
76. Schultze-Lutter F, Ruhrmann S, Hoyer C, Klosterkötter J, Leweke FM (2007) The initial prodrome of schizophrenia: different duration, different underlying deficits? *Compr Psychiatry* 48:479–488
77. Segonne F, Dale AM, Busa E, Glessner M, Salat D, Hahn HK, Fischl B (2004) A hybrid approach to the skull stripping problem in mri. *NeuroImage* 22:1060–1075
78. Semple DM, Ramsden F, McIntosh AM (2003) Reduced binocular depth inversion in regular cannabis users. *Pharmacol Biochem Behav* 75:789–793
79. Sheffield JM, Barch DM (2016) Cognition and resting-state functional connectivity in schizophrenia. *Neurosci Biobehav Rev* 61:108–120
80. Sled JG, Zijdenbos AP, Evans AC (1998) A nonparametric method for automatic correction of intensity nonuniformity in mri data. *IEEE Trans Med Imaging* 17:87–97
81. Smith GN, Thornton AE, Lang DJ, MacEwan GW, Kopala LC, Su W, Honer WG (2014) Cortical morphology and early adverse birth events in men with first-episode psychosis. *Psychol Med* 45(9):1825–1837. <https://doi.org/10.1017/S003329171400292X>
82. Storsve AB, Fjell AM, Tamnes CK, Westlye LT, Overbye K, Aasland HW, Walhovd KB (2014) Differential longitudinal changes in cortical thickness, surface area and volume across the adult life span: regions of accelerating and decelerating change. *J Neurosci* 34:8488–8498
83. Taylor SF, Kang J, Brege IS, Tso IF, Hosanagar A, Johnson TD (2012) Meta-analysis of functional neuroimaging studies of emotion perception and experience in schizophrenia. *Biol Psychiatry* 71:136–145
84. Thayer RE, Hagerly SL, Sabbineni A, Claus ED, Hutchison KE, Weiland BJ (2016) Negative and interactive effects of sex, aging,

- and alcohol abuse on gray matter morphometry. *Hum Brain Mapp* 37:2276–2292
85. Uddin LQ, Kaplan JT, Molnar-Szakacs I, Zaidel E, Iacoboni M (2005) Self-face recognition activates a frontoparietal “mirror” network in the right hemisphere: an event-related fMRI study. *NeuroImage* 25:926–935
 86. Vijayakumar N, Allen NB, Youssef G, Dennison M, Yucel M, Simmons JG, Whittle S (2016) Brain development during adolescence: a mixed-longitudinal investigation of cortical thickness, surface area, and volume. *Hum Brain Mapp* 37:2027–2038
 87. Wang J, Yang Y, Fan L, Xu J, Li C, Liu Y, Fox PT, Eickhoff SB, Yu C, Jiang T (2015) Convergent functional architecture of the superior parietal lobule unraveled with multimodal neuroimaging approaches. *Hum Brain Mapp* 36:238–257
 88. Watanuki T, Matsuo K, Egashira K, Nakashima M, Harada K, Nakano M, Matsubara T, Takahashi K, Watanabe Y (2016) Precentral and inferior prefrontal hypoactivation during facial emotion recognition in patients with schizophrenia: a functional near-infrared spectroscopy study. *Schizophr Res* 170:109–114
 89. Woo CW, Krishnan A, Wager TD (2014) Cluster-extent based thresholding in fMRI analyses: pitfalls and recommendations. *NeuroImage* 91:412–419
 90. Yuan X, Han Y, Wei Y, Xia M, Sheng C, Jia J, He Y (2016) Regional homogeneity changes in amnesic mild cognitive impairment patients. *Neurosci Lett* 629:1–8
 91. Zilles K, Palomero-Gallagher N, Amunts K (2013) Development of cortical folding during evolution and ontogeny. *Trends Neurosci* 36:275–284
 92. Zipursky RB, Lim KO, Sullivan EV, Brown BW, Pfefferbaum A (1992) Widespread cerebral gray matter volume deficits in schizophrenia. *Arch Gen Psychiatry* 49:195–205